Chemical Science

Accepted Manuscript

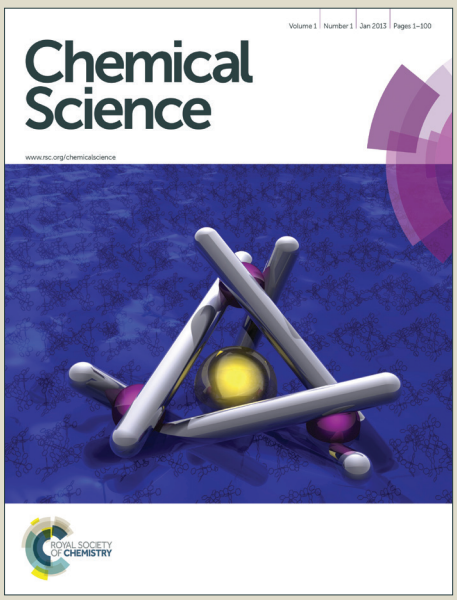

ROYAL SOCIETY OF CHEMISTRY

www.rsc.org/chemicalscience

Journal Name

RSCPublishing

ARTICLE

Phosphorus(V) Tetraazaporphyrins: Porphyrinoids Showing an Exceptionally Strong CT Band between the Soret and Q Bands

Cite this: DOI: 10.1039/x0xx00000x

Received ooth January 2012,
Accepted ooth January 2012

DOI: 10.1039/x0xx00000x

www.rsc.org/

Taniyuki Furuyama,[a] Takuya Yoshida,[a] Daisuke Hashizume[b] and Nagao Kobayashi*[a]

A series of tetraazaporphyrin phosphorus(V) complexes (PTAPs) has been synthesized and characterized practically for the first time, and are found to exhibit unique absorption properties not observed for normal porphyrinoids. The absorption spectrum of $[Ar_8TAPP(OMe)_2][ClO_4]$ shows a broad, intense band between the Soret and Q bands at around 530 nm, differing from the typical metalloTAPs and phthalocyanine phosphorus(V) complexes (PPcs). Both electron donating and withdrawing substituents affect the complete absorption envelope of the PTAPs, even though the substituents lie outside the TAP π conjugation system. Moreover, the trends across the entire absorption range correlate well with the Hammett constants corresponding to the substituents. Magnetic circular dichroism (MCD), cyclic voltammetry (CV) and theoretical calculations using density functional theory (DFT) were performed to interpret the unique absorption properties of PTAPs. The interaction between the aryl substituents and the TAP macrocyclic core could be estimated by carefully taking into account the results of spectroscopies and frontier molecular orbitals. The effect of the phosphorus(V) ion in TAP was found to be stronger than that in Pc. In TAP, the phosphorus(V) ion intensifies a charge-transfer (CT) band from peripheral aryl moieties to the TAP core. The band deconvolution analysis of the absorption and MCD spectra also clarified the effect of phosphorus(V) ion. The combination of a main-group element (phosphorus) and macrocyclic core (TAP) appears useful for developing new organic materials which absorb over the complete UV-visible region (300-700 nm) as a single, discrete compound.

Introduction

The development of organic dyes and pigments is an established, but notable area in current material chemistry fields, such as dye-sensitized solar cells (DSSCs),[1] organic field-effect transistors (OFETs),[2] organic photovoltaics (OPVs),[3] photosynthesis,[4] and chemical sensors.[5] Tuning of the color is one of the most important topics in this area, since the functional properties of dyes often correlate with their color. For example, organic dyes in an efficient DSSC must have broad, intense absorption in the UV and visible regions, and several materials have been proposed for generating a large photocurrent response.[6] Phthalocyanines (Pcs, Scheme 1), the congeners of tetraazaporphyrins (TAP), are some of the most promising dyes for applications in various fields, because of their high stability and intense absorption band in the UV and visible regions (termed the Soret and Q bands). Changing the absorption properties of Pcs is one of the most attractive research topics in their chemistry, since novel Pcs having new absorption properties may produce new functionalities. A number of Pcs with modifications of their peripheral substituents and/or the nature of the π conjugation system have been synthesized with the aim of tailoring the absorption envelope.[7] However, the development of novel strategies for rationally designing the absorption properties of Pc by simple synthetic methods remains a challenge in the chemistry of organic dyes and related materials. Recently, we reported that phosphorus(V) Pc complexes (PPcs), synthesized as highly-stable materials in a few steps, absorb strongly in the near-IR region beyond 1000 nm.[8] Interestingly, the extent of the red shift upon phosphorus insertion into the core of the Pc was different from substituent to substituent.[9] Hence, the combination of a central phosphorus ion, peripheral substituents, and the Pc core appears crucial, in order to obtain novel absorption properties.

In this paper, we have synthesized and studied tetraazaporphyrin phosphorus complexes (PTAPs) having eight aryl groups at peripheral positions (Scheme 1). The Q band of TAP appears at shorter wavelengths (600~550 nm) due to the smaller π conjugation compared to Pcs. On the other hand, we

previously reported that the Q band of octaphenyl-substituted TAP appear at longer wavelengths (650~600 nm) than tetra-*tert*-butyl substituted TAP, by more than 40 nm,[10] showing clearly that the substitution effect at peripheral positions of TAP is stronger than for Pc, because the peripheral substituents are directly linked to the smaller TAP core. In this work, we have found that the insertion of phosphorus(V) into the TAPs can change the entire absorption envelope. Although the first PPc was synthesized over 30 years ago,[11] the synthesis of PTAPs has not been reported to date, with the exception of one paper by Goldberg *et al*.[12] They reported that PTAP was obtained in a very small yield (< 2%) as a byproduct of the synthesis of a corrolazine phosphorus(V) complex, but were unable to characterize it. The absorption envelope of TAP usually resembles that of Pc, and the absorption properties of both Pc and TAP can be interpreted similarly.[13] However, the absorption properties of PTAPs cannot be explained in direct comparison with those of PPcs. We will discuss the marked effect of the phosphorus(V) ion as a central element of TAP. A series of PTAPs containing eight *tert*-butyl (^{t}Bu)-, OMe-, F-, or CF_3-phenyl groups at peripheral positions were thus synthesized, in order to reveal the fundamental rules of the absorption properties of PTAPs.

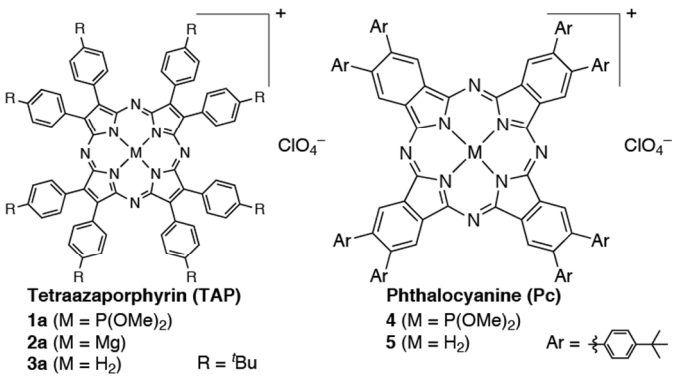

Scheme 1 Chemical structures of azaporphyrin families.

Results and discussion

Synthesis of phosphorus(V) complexes of azaporphyrinoids

The synthetic procedures for the TAPs and Pcs are shown in Scheme 2. Since it is free-base azaporphyrinoid which provides a facile access to main-group element derivatives, free-base TAPs and Pcs were first prepared according to the literature procedures in moderate yields.[7] Although free-base TAP **3** could be obtained by direct tetramerization of pyrroline-2, 5-diimine in low yield, the Mg complex **2** (MgTAP) was first synthesized using a template method, followed by demetalation using trifluoroacetic acid. For the introduction of a phosphorus ion into the center of TAPs and Pcs, phosphorus oxybromide was used as a precursor. At the end of the reaction, the reaction mixture was quenched with dichloromethane/methanol, which provided dimethoxy substituted (as axial ligand) phosphorus azaporphyrinoids. Finally, the counter anion was replaced by excess $NaClO_4$, producing the desired phosphorus complexes **1a** (TAP) and **4** (Pc) in yields of 56 and 34%, respectively, as the perchlorate salts. These phosphorus complexes showed excellent solubility in general organic solvents, and could be fully characterized by NMR and HR-MALDI-FT-ICR mass spectroscopy. For example, the ^{1}H NMR spectrum of **1a** shows only one kind of peripheral *tert*-butylphenyl group (8.26, 7.65, and 1.51 ppm), and a doublet assignable to axial methoxy groups at high field (-1.68 ppm); hence the conformation of **1a** appears to retain a highly symmetrical and non-aggregated structure in solution. Since the chemical shift of the methoxy groups appeared at higher field than the corresponding signal of **4** (-1.06 ppm), we can conclude that the shielding effect of the diatropic ring current of TAP is stronger than that of Pc, as previously pointed out in the comparison of TAP, Pc, naphthalocyanine, and anthracocyanine.[14] The ^{31}P NMR spectrum exhibited only one peak at -182 ppm, supporting hexacoordinated phosphorus representations[15] lying within the central cavity of the TAP macrocycle.

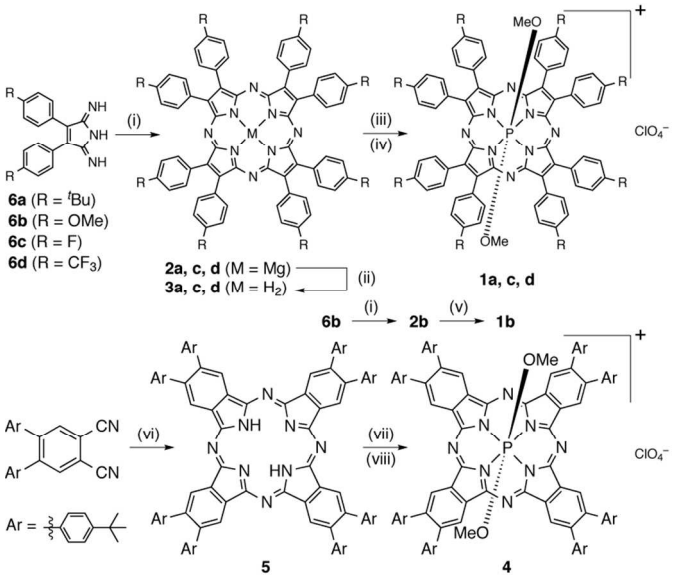

Scheme 2 Synthesis of azaporphyrin phosphorus(V) complexes. *Reagents and conditions*: (i) (^{n}BuO)$_2$Mg (0.75 eq), ^{n}BuOH, reflux, 24 h, 62-95%; (ii) CF_3COOH, rt, 30 min, 78-86%; (iii) $POBr_3$ (50 eq), pyridine, 90°C, 15 h, then methanol, rt, 18 h; (iv) $NaClO_4$, CH_3CN/CH_2Cl_2, rt, 12 h, 15-56% (2 steps); (v) $POBr_3$ (50 eq), pyridine, reflux, 15 min, then methanol, rt, 12 h, 6%; (vi) ^{n}BuOLi, ^{n}BuOH, reflux, 1 h, 77%; (vii) $POBr_3$ (40 eq), pyridine, rt, 24 h, then $MeOH/CH_2Cl_2$, rt, 30 min; (viii) $NaClO_4$, CH_2Cl_2, rt, 18 h, 33% (2 steps).

Finally, the structure of **1a** was unambiguously elucidated by X-ray diffraction analysis of crystals obtained from the diffusion of *n*-hexane into a 1,2-dichloroethane solution of **1a** (Fig. 1).‡ The TAP macrocycle of **1a** has a ruffled structure, similarly to phosphorus(V) Pc.[8] However, the degree of distortion of the core (Δr) of **1a** (0.26) is smaller than that of P(V)Pc (Δr = 0.43). The distance between the two pyrrole-nitrogen atoms at opposite sides in the core (3.68 Å) is shorter than those of typical metalloTAPs (3.8~3.9 Å).[16] Hence, it appears that the small atomic radius (106 pm) of phosphorus(V) has produced the ruffled structure of PTAP. The tilt angle between the peripheral aryl groups and macrocycle is another important structural characteristic. The angle can be derived from the dihedral angles of aryl groups with respect to the plane defined by the pyrrole moiety of the TAP to which they are attached. The average tilt angle in **1a** is 41.0° in the 37.7° to 44.0° range, which is in-between that of decaaryl-superazaporphyrin[17] (45.9°) and hexaaryl-subporphyrazine[18] (40.4°). The influence of peripheral aryl substituents on the

electronic structure of the macrocyclic core is generally considered to be larger the smaller the tilt angle. Although this influence is discussed in a later section, from the above tilt angle values, the influence appears to be larger for subporphyrins,[19] subporphyrazine and **1a** rather than for superazaporphyrins. Since **1a** has two axial ligands and bulky peripheral substituents, almost no TAP–TAP packing interaction was considered to exist.

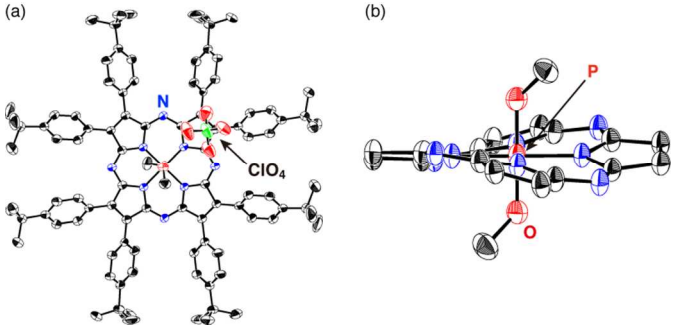

Fig. 1 X-ray crystal structure of **1a**. The thermal ellipsoids were scaled to the 50% probablility level. (a) top view; (b) side view (peripheral substituents and counteranion were omitted). In both views, hydrogen atoms and solvent molecules have been omitted for clarity.

PTAPs endowed with either an electron donor (**1b**) or acceptor (**1c**, **d**) were also synthesized using a similar procedure. However, the solubility of **1c** and **1d** was very low after the counter anion was replaced, so that they were characterized only by absorption, NMR and HR-MS spectra, and samples containing a mixture of counter anions were used for analysis. The envelope of the absorption bands did not depend on the counteranion for **1a**; hence we can conclude that the counteranion does not affect the electronic structure of PTAPs (Fig. S1).

UV-Visible and MCD Spectra

In order to compare the effect of the phosphorus(V) ion between PTAP and PPc, UV-vis absorption spectra of free-bases, magnesium (metal) complexes, and phosphorus(V) complexes are shown in Fig. 2a (TAPs) and Fig. 2b (Pcs). Free-base TAP **3a** has two intense absorption peaks in the visible region (671 and 606 nm) which can be assigned to the Q_x and Q_y bands, supported by the corresponding MCD spectrum of opposite sign. The UV-vis spectrum of MgTAP **2a** is characteristic of metallated TAPs with D_{4h} symmetry, and the Q band appears approximately halfway between the split Q band of **3a**. Both **2a** and **3a** exhibit a weak band at around 460 nm, with an associated Faraday *A* term (for **2a**) or two Faraday *B* terms (for **3a**) in the corresponding MCD spectra. As already reported by our group[10] and others,[20] these bands can be assigned to a n–π* transition from the lone-pair of *meso* nitrogen atoms to the LUMO of the TAP macrocycle. Because the n–π* transition is originally forbidden, this band is barely observed in the case of *tert*-butylated TAPs.[10] As can be deduced from the discussion in the section on MO calculations, we can conclude that the peripheral aryl groups have enhanced the CT character, so that and the intensity is increased for aryl-substituted MgTAPs. However, the absorption coefficient of this peak of **2a** is still small (< 1.0 x 10^4 $M^{-1}cm^{-1}$).

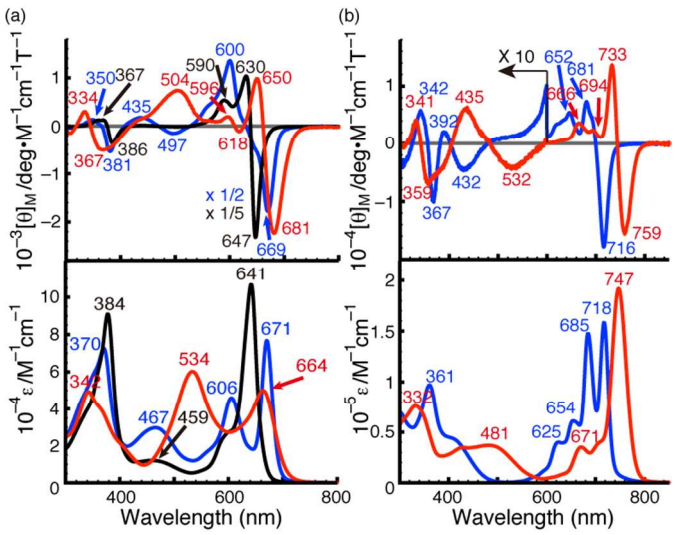

Fig. 2 (a) UV-vis absorption (bottom) and MCD (top) spectra of **1a** (red), **2a** (black), and **3a** (blue) in CH_2Cl_2. (b) UV-vis absorption (bottom) and MCD (top) spectra of **4** (red) and **5** (blue) in CH_2Cl_2.

Interestingly, the absorption envelope of PTAP **1a** is quite different from those of free-base **3a** and the Mg complex **2a**. A Q band-like absorption was observed at 664 nm, and the phosphorus(V) ion assisted slightly to shift the position of the Q band. The envelope of the Soret band resembles that of the free-base and Mg complexes, with a peak appearing at 342 nm. However, a broad, intense absorption band appeared between the Soret and Q bands at 534 nm for only PTAP. Therefore, **1a** can absorb across the entire UV-visible region (in particular, the absorption coefficient is more than 2 x 10^4 $M^{-1}cm^{-1}$ across 500-700 nm in CH_2Cl_2) as a single chromophore. The color of a solution of **1a** in dichloromethane is purple rather than the typical green color of aryl-substituted free-base and metallated TAPs. In the MCD spectrum of **1a**, typical Faraday *A* terms were detected for both the Soret (367 and 334 nm) and Q band (681 and 650 nm) regions, in agreement with the approximate D_{4h} symmetry of **1a** in solution. The absorption band at 534 nm cannot, of course, be assigned to the Q band, and its position is close to that of a n-π* CT transition (from the non-bonding lone pair electron of *meso*-nitrogen to the LUMO of the TAP skeleton) in **2a** and **3a**, but the apparent intensity is about 2-4 times stronger. The MCD spectrum corresponding to the 534 nm absorption cannot be interpreted simply, since the complex feature suggests an overlap of several transitions. The detailed assignment and properties of this band will be discussed later.

The absorption envelope of PPc **4** is somewhat different from that of PTAP **1a**, resembling those of regular metallated Pcs with directly linked phenyl groups. A single, intense Q band appeared at 747 nm, which is about 30 nm to longer wavelength than that of tetra-*tert*-butylated PPc[8a] (716 nm in $CHCl_3$), so that we can conclude that the *tert*-butylphenyl groups of **4** marginally affect the spectroscopic properties of the Pc. The Faraday *A* MCD term of **4** in this region further indicates that the practical chromophore symmetry of this complex is close to D_{4h}. The red-shift induced by phosphorus ion insertion (i.e. the Q-band shift on going from **5** to **4**) was not large (ca. 870 cm^{-1}).

Electrochemistry

Cyclic voltammograms of PTAP **1a**, MgTAP **2a**, free-base TAP **3a**, PPc **4**, and free-base Pc **5** were measured in *o*-dichlorobenzene (*o*-DCB), with representative voltammograms shown in Fig. 3. It is well established for Pcs and TAPs that the potential difference between the first oxidation and reduction potentials ($E_{1ox} - E_{1red}$) is well correlated with the lowest transition energies.[21] Free-base TAP **3a** has two reduction (at -1.16 and -1.45 V) and one oxidation (at 0.76 V) process, while free-base Pc **5** showed two reduction couples at -1.34 and -1.61 V, and its first oxidation at 0.30 V. The value of $E_{1ox} - E_{1red}$ increases in going from Pc (1.64 V) to TAP (1.92 V), as anticipated from the molecular size and the position of the Q band. The voltammogram of MgTAP **2a** was typical of that of metalloTAPs. After the introduction of phosphorus into the TAP, the first reduction couple shifted to -0.40 V, which is an anodic shift of 0.76 V compared with the first reduction couple (-1.16 V) of the free-base species **3a**. A similar 0.76 V anodic shift was also observed in the case of Pcs, such that on going from free-base Pc **5** to its phosphorous complex **4**, the first reduction potential shifted from -1.34 to -0.58 V. The first oxidation potential of PPc **4** appeared at 0.90 V, which is an anodic shift of 0.60 V on phosphorous(V) insertion. The ($E_{1ox} - E_{1red}$) value of PPc **4** is 1.48 V compared with 1.64 V for the corresponding free-base **5** and 1.70 V for $^{t}Bu_4PcH_2$.[17] The first oxidation of PTAP **1a** was not detected within the window limit of the solvent (ca. 1.2 V). Since the first oxidation is the process for removing an electron from the HOMO, while the first reduction is the process for adding an electron to the LUMO, these voltammetric results indicate that both the LUMO and HOMO are markedly stabilized by the strongly electron-withdrawing phosphorus(V) ion. However, the unique absorption spectrum of **1a** could not be explained only by these electrochemical results.

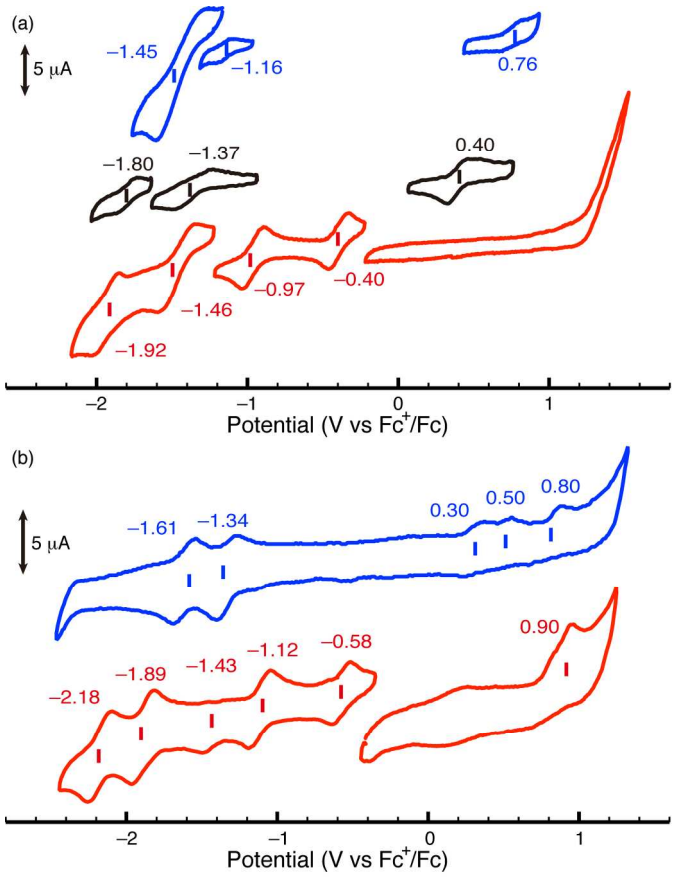

Fig. 3 Cyclic voltammetry data for (a) **1a** (red), **2a** (black), and **3a** (blue) and (b) **4** (red) and **5** (blue). Cyclic voltammograms were recorded in 0.5 mM solutions of analyte in 0.1 M $^{n}Bu_4NClO_4$/*o*-DCB. Ferrocene was used as an internal standard and set to 0 V.

Estimation of peripheral substitution effects of PTAPs

In order to examine the properties of the CT-like band at 534 nm of PTAP **1a**, a series of PTAPs with *para*-substituted aryl moieties were prepared (*para* position was either ^{t}Bu, OMe, F, or CF_3). The absorption spectra of substituted PTAPs **1a–d** and ^{t}Bu-MgTAP **2a** are shown in Fig. 4, with the absorption parameters summarized in Table 1. Both the Q and the CT-like bands appeared, depending on the substituents, over a wide range of the visible region, although the absorption properties of arylated porphyrinoids (*meso*-aryl[22] and/or β-aryl[23] porphyrins, subphthalocyanines,[24] and superazaporphyrins[17]) do not generally depend on the substituent at the aryl moiety. As previously reported,[20, 25] the absorption spectra of MgTAPs **2a–d** are only slightly perturbed by the substituents in the region between the Soret and Q bands (Fig. S2). Thus, the comparison between the spectra of substituted PTAPs **1a–d** and MgTAPs **2a–d** indicates that the central phosphorus ion enhances the substituent effect even though the substituents are located at the *para* positions of the phenyl groups, outside the π conjugation system of the TAP.

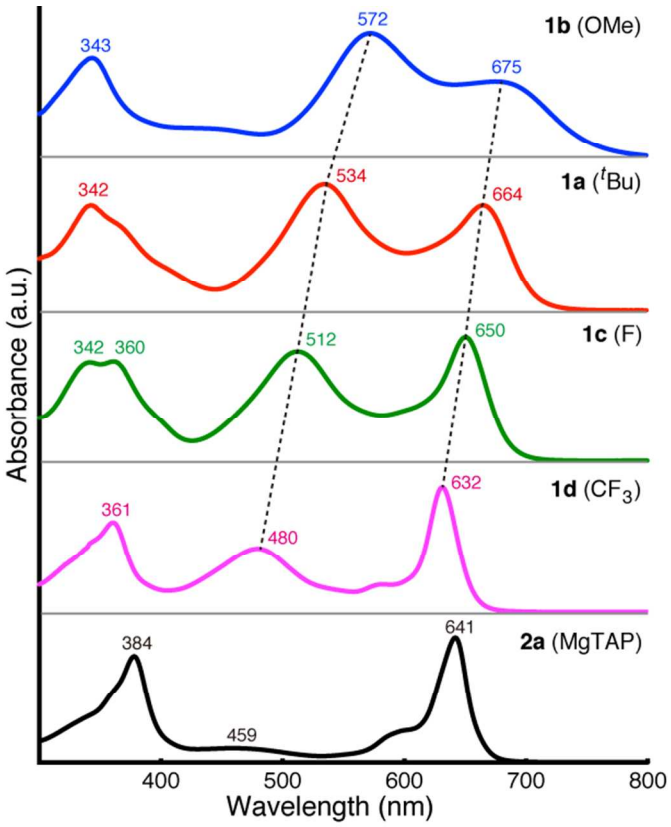

Fig. 4 UV-vis absorption spectra of **1a**-**d** and **2a** in CH_2Cl_2.

Table 1 Summary of absorption properties of PTAPs in CH_2Cl_2.

Compound	σ_p	λ_{CT} (nm) [a]	λ_Q (nm) [b]	A_Q/A_{CT} [c]
1a (^{t}Bu)	−0.20	534	664	0.83
1b (OMe)	−0.27	572	675	0.62
1c (F)	0.06	512	650	1.13
1d (CF_3)	0.54	480	632	1.97

[a] Position of peak in the CT band region (550-450 nm). [b] Position of peak in the Q band region (700-600 nm). [c] Ratio of intensities of Q band to CT band.

The difference of the CT-like bands between electron withdrawing (CF_3, **1d**) and electron donating (OMe, **1b**) groups (92 nm, 3400 cm^{-1}) was larger than that of the Q bands (43 nm, 1000 cm^{-1}). The small difference for the Q band suggests that the peripheral substituents only marginally affect the electronic structure of the HOMO and LUMO. On the other hand, the peaks at around 550~450 nm apparently contain a transition associated with the aryl moiety, since they change in both intensity and position depending on the substituents at the *para* positions of the phenyl groups, suggesting that they are CT bands between the aryl moiety and the TAP core. PTAPs **1a-b** containing electron-donating groups have a Q-band intensity smaller than that of the CT bands, while PTAPs **1c-d** containing electron-withdrawing groups display the opposite absorption properties, where the intensity of the Q bands are larger than the CT bands. For example, in the case of the CF_3-substituted PTAP **1d**, the Q band is sharp and intense, while the CT-like band is relatively small, resembling that of typical metalloTAPs (i.e. **2a**). Since similar phenomena were observed in the case of tetraazachlorin-fullerene conjugates,[26] the electronic communication between the peripheral aryl moieties and PTAP core was inferred to be altered by the substituents. More interestingly, both the position and intensity of the peaks of PTAPs exhibit a noteworthy correlation with the Hammett σ_p value[27] of substituents on the aryl moieties (Fig. 5). Plots of the position of both the Q and the CT-like bands versus the Hammett σ_p value of the substituents constitute a straight line for **1a-d**. Plots of the ratio of the intensity of the Q bands to that of the CT bands versus the Hammett σ_p value of the substituents also constitute a good straight line. Hence, the Hammett σ_p value can be useful in fashioning new PTAPs designed to access appropriate properties in various fields.

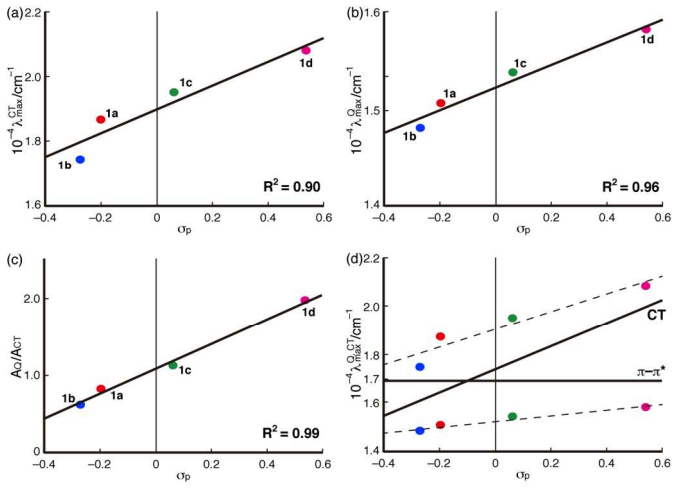

Fig. 5 Plots of (a) position of the CT bands, (b) position of the Q bands, and (c) ratio of A_Q to A_{CT} versus Hammett σ-values derived from the PTAPs. (d) Configuration interaction diagrams for the CT and Q transitions.

Finally, we performed a spectral deconvolution analysis of the absorption and MCD spectra[28] of MgTAP (**2a**) and PTAP (**1a**), as a representative case to provide a quantitative estimate of the energies of the band centers and the magnitudes of the Q and CT bands. Identical bandwidths and centers were used to fit the MCD and absorption spectra. Fig. 6 displays the results of the band deconvolution in the Q and CT band regions, with the band properties summarized in Table 2. The absorption and MCD spectra of both TAPs in this region could be interpreted as a sum of 15 Gaussian curves, which is reasonable for normal azaporphyrins. MCD Faraday *A* terms were required for the Q_{00} and CT bands. The MCD intensity of the CT bands was very weak due to the small changes of orbital angular momenta between the ground and excited states. The CT bands were assigned carefully based on an inflection point in the MCD spectrum (Fig. S3). While the area (intensity) of the Q_{00} band is similar between **1a** (4.29 x 10^7 $M^{-1}cm^{-2}$) and **2a** (5.02 x 10^7 $M^{-1}cm^{-2}$), the area of the CT band of **1a** (4.24 x 10^7 $M^{-1}cm^{-2}$) is about 7 times larger than that of **2a** (7.2 x 10^6 $M^{-1}cm^{-2}$). The CT band of **1a** (534 nm) appeared at longer wavelength than that of **2a** (486 nm), supporting the conclusion that the phosphorus(V) ion affects not only the intensity, but also the position of the CT band.

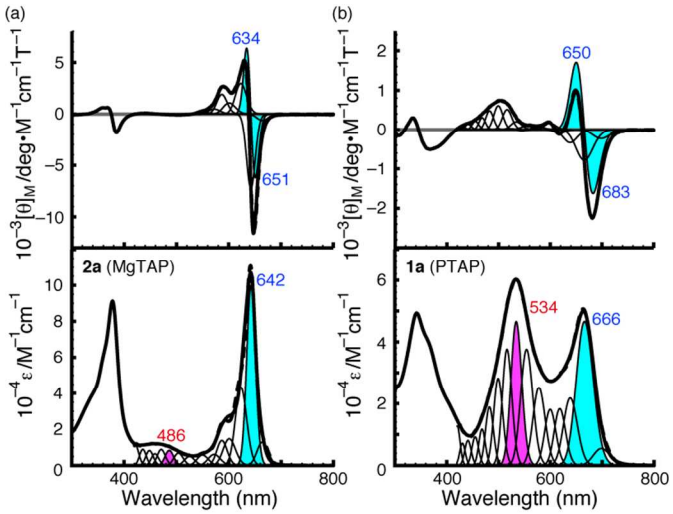

Fig. 6 UV-vis absorption (bottom) and MCD (top) spectra of **2a** (a) and **1a** (b) in CH_2Cl_2. Deconvoluted Gaussian curves and the simulated spectra are shown by the black solid lines and broken line with the Q_{00} and CT bands denoted by the blue and red colored Gaussian curves, respectively.

Table 2 Summary of parameters of band deconvolution analysis.

Compd	Assign.	λ (nm)	fwhm (cm^{-1})	Intensity (10^4•$M^{-1}cm^{-1}$)	Area (10^7•$M^{-1}cm^{-2}$)
1a	Q	666	834	4.66	4.29
	CT	534	805	4.66	4.24
2a	Q	642	460	9.97	5.02
	CT	486	803	0.84	0.72

Computational studies

In order to enhance the interpretation of the electronic structures of PTAP and understand the effect of the central phosphorus ion and peripheral substituents, MO calculations of model TAPs, **1e** (phosphorus(V) complex) and **2e** (magnesium complex), have been performed, where peripheral substituents were replaced with phenyl groups for simplicity. The molecular geometries were first optimized at the DFT level using the B3LYP/6-31G(d), as implemented in Gaussian 09.[29] The optimized structures agree with the structures obtained from the experimental spectroscopies. The P(V) complex **1e** has a deformed structure similar to the crystallographic structure of **1a** and PPc,[8] while the Mg complex **2e** revealed a planar structure similar to normal metalloTAPs.[17] However, the calculated stick absorption spectrum of **2e** with the same method did not reproduce the experimental spectrum of **2a**. Since the absorption properties and electronic structures of MgTAP have been studied sufficiently,[13, 30] this problem appears to have been caused by the choice of the calculation level of TDDFT. Therefore, we also conducted similar calculations using several theories and basis sets, and found that the LC-BLYP[31]/6-31G(d) level improved the estimation of the experimental peaks (Fig. S4). Consequently, we applied the LC-BLYP method to the calculations for the molecular orbitals and excited states of **1e** and **2e**.

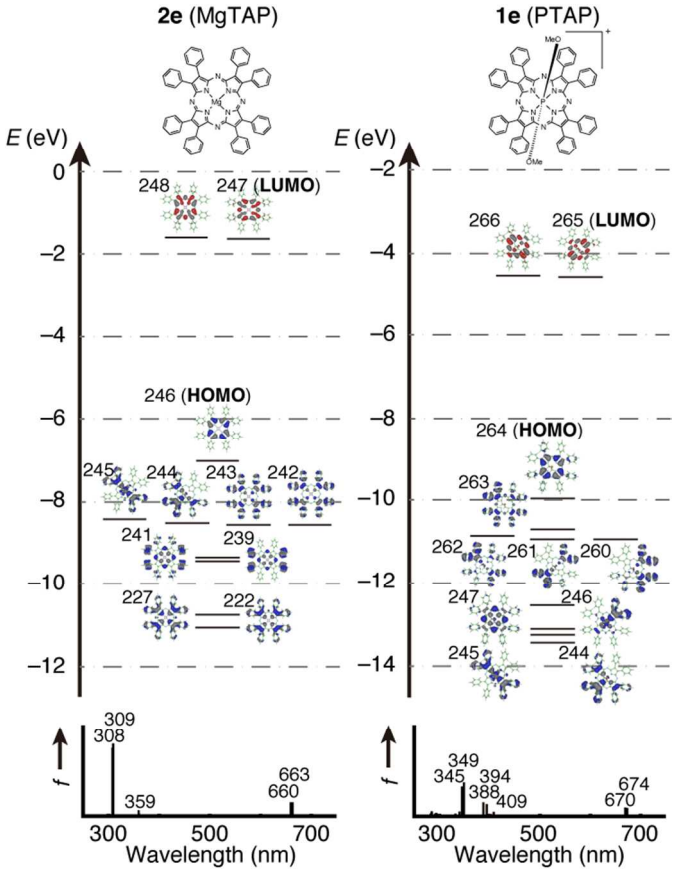

Fig. 7 Partial molecular energy diagram and orbitals of Ph_8TAPs (**1e** and **2e**) (top) and their calculated absorption spectra (bottom). Blue and red plots indicate occupied and unoccupied MOs, respectively. Calculations were performed at the LC-BLYP/6-31G*//B3LYP/6-31G* level (for details, see the SI).

Partial MO energy diagrams of the model structures are shown in Fig. 7, with the results of TDDFT calculations summarized in Table S2. The typical absorption properties of TAPs have been successfully explained by Gouterman's "four-orbital" model,[32] and hence we attempted to interpret the MO diagrams with this model. For both TAPs, the HOMO, LUMO, and LUMO+1 are dominated by the TAP orbitals, and these orbitals corresponded to the a_{1u}, e_{gy}, and e_{gx}-like orbitals in Gouterman's model, respectively. Therefore, these calculated transitions at 674 and 670 nm (for P(V)TAP **1e**) and 663 and 660 nm (for MgTAP **2e**) can be assigned to the experimental Q bands. In the UV region of the calculated spectrum of **2e**, two close, intense bands were obtained at 309 and 308 nm, energetically comparable to the observed Soret bands. These bands are composed of transitions from the HOMO-1, HOMO-2, HOMO-3, HOMO-4, HOMO-5, and HOMO-7 to the LUMO and LUMO+1 (almost degenerate), and particularly from the HOMO-1 to the degenerate LUMOs. The HOMO-1 to HOMO-7 are delocalized over the entire complex, indicating that the intramolecular charge transfer (CT) transitions including phenyl (or aryl) moiety are not negligible for these bands. However, the TAP moiety of the HOMO-1, HOMO-5, and HOMO-7 originate from the a_{2u} type orbitals. The band calculated at 359 nm is relatively weak, composed of transitions from the HOMO-1~7, HOMO-19, and HOMO-24 to the degenerate LUMOs. The HOMO-19 and HOMO-24 are partially localized on the lone pairs of the *meso*-nitrogens, supporting the

conclusion that these transitions have some n-π* transition character. This assignment is also supported by previous calculations,[20a] and the weak band of **2a** at 459 nm is therefore assigned ambiguously to an n-π* transition. The aryl moieties also contribute to these bands, and the contribution of the CT transition is crucial for the intensity of this band.

The introduction of the phosphorus(V) ion into the TAP center stabilizes the entire MOs, but do not affect the symmetry of the HOMO, LUMO, and LUMO+1. The calculated HOMO-LUMO energy gap of P(V)TAP **1e** is similar to that of MgTAP **2e**, so that we can infer that the position of the Q band of **1a** changes slightly when the phosphorus(V) ion is introduced. In the region between 450 and 350 nm, the calculated transitions (409, 403, 394, and 388 nm) of **1e** are more complex than those of **2e**. The MCD spectrum of **1a** was quite complicated at around 500 nm, while that of **2a** showed a clear Faraday *A* term at 509 and 444 nm. Thus, these experimental differences appeared to be reproduced by this calculation on **1e**, due perhaps to the deformation of the macrocycle and/or a weak interaction between phosphorus(V) and the TAP core. These transitions comprise the n-π* transitions and CT transitions, as mentioned for the magnesium complex **2e**. Moreover, these bands were estimated to be stronger than those of **2e** in the longer wavelength region. The contribution of the HOMO-1~4 dominates, and as can be judged from the size of the coefficient of MOs in Fig. 7, the MOs are mainly localized on the peripheral phenyl groups. These results reproduce clearly the experimental absorption spectrum of **1a**, where the intense CT band appears in the longer wavelength region compared to **2a**. The results of the band deconvolution analysis of **1a** and **2a** (Fig. 6) also support the calculated absorption spectra. The unique substitution effect of PTAPs can therefore be explained, since the electronic structure of the peripheral moieties affect the position and intensity of the CT band. In other words, the absorption features of **1e** can be interpreted as typical metalloTAPs, but where the position and intensity of CT bands have been markedly altered after the introduction of the phosphorus(V) ion, which enhances the absorption coefficients in the mid-visible region.

In order to examine the difference between PTAP and PPc systems, the molecular orbitals and absorption spectrum of β-$Ph_8PcP(OMe)_2$ (**4'**) were also calculated (Fig. S5), with the results showing the presence of CT transitions from the peripheral phenyls to the Pc macrocycle in the longer wavelength tail of the Soret band. The experimental broad band of **4** at 481 nm (Fig. 2b, bottom) is therefore assigned to a CT transition. However, the calculated CT transitions of PPc were weaker than those of PTAP, while the positions of these transitions were estimated in a shorter wavelength region (336-356 nm) than those of PTAP (388-409 nm). Therefore, the effect of the phosphorus(V) ion is relatively weak in β-aryl-substituted Pcs, and hence the choice of macrocycle can be seen to be essential for the unique absorption property to appear.

Finally, we would like to interpret the relationship between the CT and Q bands theoretically. Here, if we accept the above MO calculation results (Fig. 7 and Table S2) and experimental data shown in Figs. 4 and 5, we can consider as follows. The Q excited state is of E_u symmentry (we use the notation of D_{4h} symmetry). The CT excited state appears to be also of E_u symmetry, since the CT transitions are mostly from a_{1u} and a_{2u}-type orbitals delocalized over the whole molecule, including the phenyl groups, to the TAP-centered e_{gx} and e_{gy} orbitals, leading to two E_u excited states. Thus, the Q and CT transitions can arise from configuration interaction between a CT state and a π–π* state. In order to show this, we have plotted, in Fig. 5d, the CT and Q band position, together with the estimated energy of the pure π–π* state (horizontal continuous line) and the hypothetical CT state (continuous straight line of unit slope). If these states mix through configuration interaction, the experimental points should lie on the broken lines. The points in Fig. 5d appear to be consistent with this model. The positions of the straight lines are only guesses, but the overall picture seems to be essentially correct. A similar explanation was previously adopted to explain the relationship between the CT and Q bands of ferric high-spin hemoproteins.[33]

Conclusions

A series of tetraazaporphyrin phosphorus(V) complexes has been prepared practically for the first time. The phosphorus(V) ion perturbs the electronic absorption properties of TAP, while the absorption properties of the phthalocyanine phosphorus(V) complexes resemble those of metallated Pcs. Substitution at the peripheral phenyl groups can alter the position and intensity of the intense CT band lying between the Soret and Q bands. The trends across the entire absorption envelope correlate well with the Hammett constants corresponding to the substituents. The unique absorption properties could be clearly explained by both experimental band deconvolution analysis and theoretical analysis, and similar electronic structures between metalloTAP and PTAP were estimated. Based on the combination of spectroscopic and theoretical results, the effect of the phosphorus(V) ion in TAP was found to be an enhancement of a CT band between the Soret and Q bands, without perturbing the π conjugated system of the TAP. The PTAPs can absorb light across the entire UV-vis region, while the position and intensity of these absorption envelopes can be tuned rationally. This methodology provides a useful tool for manipulating the absorption properties with simple chromophores and main group elements, so that these molecules can be new candidates for functional optical materials.

Acknowledgements

This work was partly supported by the Grant-in-Aids for Scientific Research on Innovative Areas (Nos. 25109502 (NK) and 25109543 (DH), "Stimuli-responsive Chemical Species"), Scientific Research (B) (No. 23350095 (NK)), Challenging Exploratory Resarch (No. 25620019 (NK)) and Young Scientist (B) (No. 24750031 (TF)) from the Ministry of Education, Culture, Sports, Science, and Technology (MEXT). Some of the calculations were performed using the supercomputing resources at the Cyberscience Center of Tohoku University.

Notes and references

[a] *Department of Chemistry, Graduate School of Science, Tohoku University, Sendai 980-8578, Japan.*

E-mail: nagaok@m.tohoku.ac.jp; Tel: +81 22 795 7719

[b] *Materials Characterization Support Unit, RIKEN Center for Emergent Matter Science (CEMS), 2-1 Hirosawa, Wako-shi, Saitama 351-0198, Japan*

† Electronic Supplementary Information (ESI) available: Additional spectroscopic data, full details of experimental and calculation procedures for all studied compounds. CCDC 984631. For ESI and crystallographic data in CIF or other electronic formats see See DOI: 10.1039/b000000x/

‡ Crystallographic data for **1a**•6 ($C_2H_4Cl_2$): $C_{98}H_{110}N_8O_2P$•ClO_4•6($C_2H_4Cl_2$), M_w = 2156.06, monoclinic, space group *C*2/*c* (no. 15), *a* = 43.4252(18), *b* = 8.3330(4), *c* = 36.214(2) Å, *β* = 113.9416(18)°, *V* = 11976.9(11) Å^3, *Z* = 4, D_X = 1.196 Mg m^{-3}, *T* = –

183°C, μ(Mo $K\alpha$) = 0.365 mm^{-1}. $R(F)$ = 0.0689, $wR(F^2)$ = 0.1951, and S = 0.943 for 6078 reflections with $I > 2\sigma(I)$. $\Delta\rho_{min, max}$ = –0.35, 0.58 e Å^{-3}. CCDC 984631. The data can be obtained free of charge from the Cambridge crystallographic data centre *via* http://www.ccdc.cam.ac.uk/products/csd/request/

1 R. K. Kanaparthi, J. Kandhadi and L. Giribabu, *Tetrahedron.* 2012, **68**, 8383.

2 (*a*) J. Mei, Y. Diao, A. L. Appleton, L. Fang and Z. Bao, *J. Am. Chem. Soc.* 2013, **135**, 6724; (*b*) S. Allard, M. Forster, B. Souharce, H. Thiem and U. Scherf, *Angew. Chem. Int. Ed.* 2008, **47**, 4070.

3 (*a*) A. Leliège, P. Blanchard, T. Rousseau and J. Roncali, *Org. Lett.* 2011, **13**, 3098; (*b*) A. Hirao, T. Akiyama, T. Okujima, H. Yamada, H. Uno, Y. Sakai, S. Aramaki and N. Ono, *Chem. Commun.* 2008, 4714.

4 B. Albinsson and J. Mårtensson, *Phys. Chem. Chem. Phys.* 2010, **12**, 7338.

5 (*a*) D. T. McQuade, A. E. Pullen and T. M. Swager, *Chem. Rev.* 2000, **100**, 2537; (*b*) L. Xu, Y. Li, S. Wu, X. Liu and B. Su, *Angew. Chem. Int. Ed.* 2012, **51**, 8068; (*c*) Y. Li, L. Xu and B. Su, *Chem. Commun.* 2012, **48**, 4109.

6 (*a*) M. Kimura, H. Nomoto, H. Suzuki, T. Ikeuchi, H. Matsuzaki, T. N. Murakami, A. Furube, N. Masaki, M. J. Griffith and S. Mori, *Chem. Eur. J.* 2013, **19**, 7496; (*b*) A. Yella, H. Lee, H. N. Tsao, C. Yi, A. K. Chandiran, M. Nazeeruddin, E. Diau, C. Yeh, S. M. Zakeeruddin and M. Grätzel, *Science* 2011, **334**, 629; (*c*) S. Mori, M. Nagata, Y. Nakahata, K. Ysuta, R. Goto, M. Kimura and M. Taya, *J. Am. Chem. Soc.* 2010, **132**, 4054; (*d*) C. Mai, W. Huang, H. Lu, C. Lee, C. Chiu, Y. Liang, E. W. Diau and C. Yeh, *Chem. Commun.* 2010, **46**, 809; (*e*) Y. Hao, X. Yang, J. Cong, H. Tian, A. Hagfeldt and L. Sun, *Chem. Commun.* 2009, 4031; (*f*) J. He, G. Benkö, F. Korodi, T. Polívka, R. Lomoth, B. Åkermark, L. Sun, A. Hagfeldt and V. Sundström, *J. Am. Chem. Soc.* 2002, **124**, 4922.

7 (*a*) *The Porphyrin Handbook*; K. M. Kadish, K. M. Smith and R. Guilard, Eds.; Academic Press: San Diego, United States, 2003; (*b*) *Handbook of Porphyrin Science*; K. M. Kadish, K. M. Smith and R. Guilard, Eds.; World Scientific Publishing, Singapore, 2010; (*c*) J. Mack and N. Kobayashi, *Chem. Rev.* 2011, **111**, 281.

8 (*a*) T. Furuyama, K. Satoh, T. Kushiya and N. Kobayashi, *J. Am. Chem. Soc.* 2014, **136**, 765; (*b*) N. Kobayashi, T. Furuyama and K. Satoh, *J. Am. Chem. Soc.* 2011, **133**, 19642.

9 M. O. Breusova, V. E. Pushkarev and L. G. Tomilova, *Russ. Chem. Bull. Int. Ed.* 2007, **56**, 1456.

10 N. Kobayashi, S. Nakajima and T. Osa, *Chem. Lett.* 1992, **21**, 2415.

11 M. Gouterman, P. Sayer, E. Shankland and J. P. Smith, *Inorg. Chem.* 1981, **20**, 87.

12 B. Ramdhanie, C. L. Stern and D. P. Goldberg, *J. Am. Chem. Soc.* 2001, **123**, 9447.

13 E. J. Baerends, G. Ricciardi, A. Rosa and S. J. A. v. Gisbergen, *Coord. Chem. Rev.* 2002, **230**, 5.

14 N. Kobayashi, S. Nakajima, H. Ogata and T. Fukuda, *Chem. Eur. J.* 2004, **10**, 6294.

15 R. R. Holmes, *Chem. Rev.* 1996, **96**, 927.

16 (*a*) J. P. Fitzgerald, J. R. Lebenson, G. Wang, G. T. Yee, B. C. Noll and R. D. Sommer, *Inorg. Chem.* **2008**, *47*, 4520. (*b*) J. P. Fitzgerald, B. S. Haggerty, A. L. Rheingold, L. May and G. A. Brewer, *Inorg. Chem.* **1992**, *31*, 2006; (*c*) Y. Ni, J. P. Fitzgerald, P. Carroll and B. B. Wayland, *Inorg. Chem.* **1994**, *33*, 2029; (*d*) D. S. Bohle, P. Debrunner, J. P. Fitzgerald, B. Hansert, C.-H. Hung and A. J. Thomson, *Chem. Commun.* **1997**, 91.

17 T. Furuyama, Y. Ogura, K. Yoza and N. Kobayashi, *Angew. Chem. Int. Ed.* **2012**, *51*, 11110.

18 T. Higashino, M. S. Rodríguez-Morgade, A. Osuka and T. Torres, *Chem. Eur. J.* **2013**, *19*, 10353.

19 (*a*) S. Vancoillie, M. Hendrickx, M. T. Nguyen, K. Pierloot, A. Ceulemans, J. Mack and N. Kobayashi, *J. Phys. Chem. A* **2012**, *116*, 3960; (*b*) Y. Inokuma, Z. S. Yoon, D. Kim and A. Osuka, *J. Am. Chem. Soc.* **2007**, *129*, 4747.

20 (*a*) K. Toyota, J. Hasegawa and H. Nakatsuji, *Chem. Phys. Lett.* 1996, **250**, 437; (*b*) H. Nie, A. G. M. Barrett and B. M. Hoffman, *J. Org. Chem.* 1999, **64**, 6791.

21 A. B. P. Lever In *Phthalocyanines: Properties and Applications*; C. C. Leznoff and A. B. P. Lever, Eds.; VCH: Weinheim, Germany, 1993, **Vol. 3**, 1.

22 (*a*) A. B. Ormond and H. S. Freeman, *Dyes and Pigments* 2013, **96**, 440; (*b*) S. Zakavi, R. Omidyan, L. Ebrahimi and F. Heidarizadi, *Inorg. Chem. Commun.* 2011, **14**, 1827.

23 (*a*) K. S. Chan, X. Zhou, M. T. Au and C. Y. Tam, *Tetrahedron* 1995, **51**, 3129; (*b*) M. Friedman, *J. Org. Chem.* 1965, **30**, 859.

24 D. Dini, S. Vagin, M. Hanack, V. Amendola and M. Meneghetti, *Chem. Commun.* 2005, 3796.

25 (*a*) E. Gonca, Ü. G. Baklaci and H. A. Dinçer, *Polyhedron* 2008, **27**, 2431; (*b*) Q. Gan, F. Xiong, S. Li, S. Wang, S. Shen, H. Xu and G. Yang, *Inorg. Chem. Commun.* 2005, **8**, 285.

26 T. Fukuda, S. Masuda and N. Kobayashi, *J. Am. Chem. Soc.* 2007, **129**, 5472.

27 C. Hansch, A. Leo, and R. W. Taft, *Chem. Rev.* 1991, **91**, 165.

28 (*a*) J. Mack and M. J. Stillman, *The Porphyrin Handbook*; K. M. Kadish, K. M. Smith and R. Guilard, Eds.; Academic Press: San Diego, United States, 2003, **Vol. 16.**, 43; (*b*) J. Mack and M. J. Stillman, *J. Am. Chem. Soc.* 1994, **116**, 1292; (*c*) T. Nyokong, Z. Gasyna and M. J. Stillman, *Inorg. Chem.* 1987, **26**, 1087.

29 M. J. Frisch *et al*., *Gaussian 09, Revision C.01*, Gaussian, Inc., Wallingford, CT, 2009. See the ESI for the full list of authors.

30 T. Fukuda and N. Kobayashi, *Handbook of Porphyrin Science*, ed. K. M. Kadish, K. M. Smith and R. Guilard, World Scientific Publishing, Singapore, 2010, **Vol. 9.**, 1.

31 (*a*) H. Iikura, T. Tsuneda, T. Yanai and K. Hirao, *J. Chem. Phys.* 2001, **115**, 3540; (*b*) H. Nitta and I. Kawata, *Chem. Phys.* 2012, **405**, 93; (*c*) T. Matsumoto, H. Chang, M. Wakizaka, S. Ueno, A. Kobayashi, A. Nakayama, T. Taketsugu and M. Kato, *J. Am. Chem. Soc.* 2013, **135**, 8646.

32 M. Gouterman, *The Porphyrins*, ed. D. Dolphin, Academic Press, New York, 1978, **Vol. 3.**, Part A. 1.

33 D. W. Smith and R. J. P. Williams, *Struc. Bonding* 1970, **7**, 1.

